# Radio-Wave Propagation Into Large Building Structures—Part 1: CW Signal Attenuation and Variability

William F. Young, *Member, IEEE*, Christopher L. Holloway, *Fellow, IEEE*, Galen Koepke, *Member, IEEE*, Dennis Camell, *Member, IEEE*, Yann Becquet, and Kate A. Remley, *Senior Member, IEEE*

***Abstract*—We report on our investigation into radio communications problems faced by emergency responders in disaster situations. A fundamental challenge to communications into and out of large buildings is the strong attenuation of radio signals caused by losses and scattering in the building materials and structure. Another challenge is the large signal variability that occurs throughout these large structures. We designed experiments in various large building structures in an effort to quantify continuous wave (CW) radio-signal attenuation and variability throughout twelve large structures. We carried radio frequency transmitters throughout these structures and placed receiving systems outside the structures. The transmitters were tuned to frequencies near public safety, cell phone bands, as well as ISM and wireless LAN bands. This report summarizes the experiments, performed in twelve large building structures. We describe the experiments, detail the measurement system, show primary results of the data we collected, and discuss some of the interesting propagation effects we observed.**

***Index Terms*—Emergency responder communications, large building radio frequency propagation, radio-frequency propagation measurements.**

## I. Introduction

When emergency responders enter large structures (e.g., apartment and office buildings, sports stadiums, stores, malls, hotels, convention centers, warehouses) communication to individuals on the outside is often impaired. Cell phone and mobile-radio signal strength is reduced due to attenuation caused by propagation through the building materials and scattering by the structural components [1]–[8]. Also, the large amount of signal variability throughout the structures causes degradation in communication systems.

Here, we report on a National Institute of Standards and Technology (NIST) project to investigate the communications problems faced by emergency responders (firefighters, police and medical personnel) in disaster situations involving large building structures. The goal is to create a large body of statistical data in the open literature for improved communication system development and design. For example, these results are useful to technology advancement initiatives focused on improving public safety communications such as [9]–[11]. As part of our effort, we are investigating the propagation and coupling of radio waves into large building structures. This paper is the first part of a two-part series covering radio frequency propagation into large structures. Part 2 summarizes results from [12] where we investigate time domain and modulated signal propagation behavior into some of these same structures. The complete results for this set of measurements are found in [13].

The experiments reported here were performed in twelve different large building structures and are essentially measurements of the reduction in radio signal strength caused by penetration into the structures. These structures include four office buildings, two apartment buildings, one hotel, one grocery store, one shopping mall, one convention center, one sports stadium, and one oil refinery. In order to study the radio characteristics of these structures at the various frequencies of interest to emergency responders, we chose frequencies near public-safety and cell phone bands, as well as ISM and wireless LAN bands (approximately 50 MHz, 150 MHz, 225 MHz, 450 MHz, 900 MHz, 1.8 GHz, 2.4 GHz, 4.9 GHz).

The experiments performed here are referred to as "radio mappings." This involved carrying transmitters (or radios) tuned to various frequencies throughout the twelve structures while recording the received signal at sites located outside the building. The reference level for these data was a direct, unobstructed line-of-sight signal-strength measurement with both transmitters and receiver external to the different structures. The purpose of the radio-mapping measurements was to investigate how the signals at the different frequencies couple into the structures, and to determine the field strength variability throughout the structures.

Several previous papers, e.g., [14]–[17], have provided results on radio mapping in buildings. Others such as [18]–[27] provide results on building penetration for a few of the frequency bands discussed here. Reference [28] outlines a measurement campaign at 2.4 GHz and 5.2 GHz carried out in support of a overall system design effort, while [26] and [27] focus on measurements for public safety. With respect to the

Manuscript received December 18, 2008; revised August 10, 2009; accepted September 25, 2009. Date of publication February 05, 2010; date of current version April 07, 2010. This work was supported in part by the U.S. Department of Justice, Community-Oriented Police Services through the NIST Public-Safety Communications Research Laboratory.

W. F. Young is with Sandia National Laboratories, Albuquerque, NM 87185 USA (e-mail: wfyoung@sandia.gov).

C. L. Holloway, G. Koepke, D. Camell, Y. Becquet, and K. A. Remley are with the National Institute of Standards and Technology, Boulder, CO 80305-3328 USA (e-mail: holloway@boulder.nist.gov).

Color versions of one or more of the figures in this paper are available online at http://ieeexplore.ieee.org.

Digital Object Identifier 10.1109/TAP.2010.2041142

TABLE I
PUBLIC SAFETY COMMUNITY FREQUENCIES

| Frequency band (MHz) | Description |
|---|---|
| 30-50 | Used mainly by highway patrols. This band is currently being phased out. |
| 150-174 | Local police and fire. |
| 406-470 | Used by federal officers and others. |
| 700-800 | Used in urban areas. |
| 800-869 | Primarily urban usage. |
| 4900 | A newly allocated band with 50 MHz bandwidth for broadband data. |

breadth of our measurement campaign, [29] provides a review of similar radio propagation measurements up to 1990 within our bands of interest, and also proposes a building classification scheme. Our effort is different is several ways: (1) a wider range and number of frequencies are covered per building, (2) multiple large building structures are investigated, and (3) the walk-through path and receive site locations are selected to emulate an emergency response scenario. Hence, this work builds upon previous work designed to accurately characterize wireless RF propagation in some key environments by adding much needed data to building categories 5 and 6 in [29], and to the general body of radio propagation measurements into and within buildings.

This paper is organized as follows. Section II provides more detail on the frequencies, the transmitters, and the automated measurement system used in the radio-mapping measurements. Section III describes the different structures and details our experimental procedures for each structure. Section IV presents representative data from the complete set of results in [13]. Finally, Section V summarizes the results of these experiments and discuss some of the interesting propagation effects observed.

## II. EXPERIMENTAL PARAMETERS AND EQUIPMENT

This section covers the frequency bands, transmitter descriptions, and the receiver configurations used in the experiments.

### A. Frequency Bands

An overview of the frequencies used by the public-safety community nationwide (federal, state, and local) is given in Table I, which shows a broad range of frequencies ranging from 30 MHz to 4.9 GHz. The modulation scheme has historically been analog FM, but this is slowly changing to digital as Project 25 radios come online [9]. The modulation bandwidth in the VHF and UHF bands has been 25 kHz, but due to the need for additional communications channels in an already crowded spectrum, most new bandwidth allocations are 12.5 kHz. The older bandwidth allocations will gradually be required to move to narrow bandwidths to increase the user density even further. The crowded spectrum and limited bandwidth are also pushing the move to higher frequency bands in order to support new data-intensive technologies. The cellular phone bands are summarized in Table II.

As shown in Table I, frequencies currently used by public safety and other emergency responders and cellular telephones

TABLE II
CELLULAR PHONE FREQUENCIES

| Frequency band (MHz) | Description |
|---|---|
| 800 | AMPS or analog systems |
| 1900 | PCS or digital system |

TABLE III
FREQUENCY BANDS USED IN THE EXPERIMENTS

| Frequency band (MHz) | Description |
|---|---|
| 49 | Simulate a public safety band |
| 162 | Simulate a public safety band |
| 226 | Simulate a public safety band |
| 448 | Simulate a public safety band |
| 902 | Simulate a public safety or cellular phone band |
| 1830 | Simulate a cellular phone band |
| 2450 | Wireless LAN |
| 4900 | Newly allocated public safety band |

are typically below 2 GHz. New frequency allocations and systems including higher frequencies (e.g., around 4.9 GHz) will become increasingly important in the future. We chose eight frequency bands below 5 GHz, from about 50 MHz to 4.9 GHz. These include four VHF bands typically used for analog FM voice, one band used for multiple technologies (analog FM voice, digital trunked FM, and cellular telephone), one band near the digital cellular telephone band, and wireless LAN bands.

In designing an experiment to investigate the propagation characteristics into large buildings at these different frequency bands, we chose frequencies very close, but not identical, to the above bands. If frequencies were chosen in the public safety or commercial land-mobile bands, interference to the public safety and cellular systems could possibly occur. Conversely, these existing systems could interfere with our experimental setup. In addition, obtaining frequency authorizations in these bands for our experiments would have been problematic due to the intense crowding of the spectrum. To circumvent these issues, we were able to receive temporary authorization to use frequencies in the U.S. government frequency bands adjacent to these public safety bands. Table III lists the frequency bands that were used in the experiments. The lower four bands correspond to the frequencies used by the public-safety community; 902 MHz can be associated with several services including both public safety and cellular phones; 1830 MHz is near the digital cellular phone; 2450 MHz covers a wireless LAN band; 4900 MHz represents a new public safety band. The exact frequencies varied, depending on which city the experiments were performed in, to avoid RF interference.

### B. Transmitters

The design requirements for the transmitters used in the experiments discussed here were that they should (1) transmit at the frequencies listed in the tables above, (2) operate continuously for several hours, and (3) be portable.

For the four lower frequency bands (the VHF/UHF public-safety bands), off-the-shelf amateur radios were modified. The


Fig. 1. 49 to 448 MHz transmitter shown in (a),(b), and (c); 902 to 4900 MHz transmitter shown in (d).

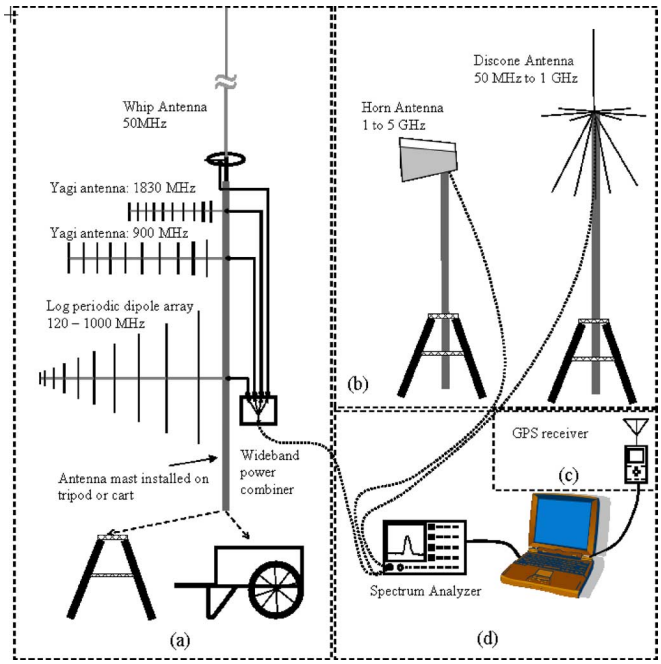


Fig. 2. Receiver equipment and setup. The initial nine experiments used antennas in (a), while the last three experiments used the antennas in (b).

modifications included (a) reprogramming the frequency synthesizer to permit transmitting at government frequencies, (b) disabling the transmitter time-out mode in order to allow for continuous transmission, and (c) connecting a large external battery pack. The modified radios and battery packs were placed in durable orange plastic cases for mobility, and the antennas were mounted on the outside of the cases. Fig. 1(a) and (b) show the final arrangement of modified transmitters used for the lower four frequency bands and Fig. 1(c) shows a closed case. Commercial transmitters already in plastic protective cases, depicted in Fig. 1(d), were available for the higher frequency bands (900 MHz, 1800 MHz, 2.4 GHz, and 4.9 GHz). The antennas had omnidirectional patterns and gains of approximately 0 dBi for the frequency bands to 1.8 GHz, and 3–5 dBi for the 2.4 and 4.9 GHz bands.

### *C. Receiving Antenna and Measurement System*

The experiments have taken place over multiple years from 2003 to present, and in conjunction with other experiments [5]–[8], [12]. This created some differences in the data collection process over time. The first four experiments collected data for all frequencies during a single walk-through, while the remaining experiments consisted of a separate walk-through for each frequency. Radio mapping of multiple frequencies on a single walk-through led to approximately 7 s between samples at each frequency. The initial single frequency per walk-through experiments enabled a data collection rate of less than 1.5 s between samples, and further refinements reduced the time between samples to approximately 0.2 s in more recent experiments.

The main components and connections of the receiving system are sketched in Fig. 2. There were two main configuration variations. For the first series of experiments, we assembled four antennas on a 4-meter mast, as illustrated in Fig. 2(a). The radio-frequency output from each antenna was fed through a 4:1 broadband power combiner. This arrangement gave us a single input to the portable spectrum analyzers, which could then scan over all the frequencies of interest without switching antennas. The four antennas were chosen to be optimal (or at least practical) for each of the frequency bands we were measuring. The selected antennas were an end-fed vertical omnidirectional antenna for 50 MHz with a gain of 4.6 dBi, a log-periodic-dipole-array (LPDA) used for the 160 MHz, 225 MHz, and 450 MHz bands with a gain of 6.7–7.1 dBi and a beamwidth of 60 degrees, and Yagi-Uda arrays for 900 MHz and 1830 MHz with gains of 15 and 13 dBi and beamwidths of 35 degrees, respectively. This assembly could then be mounted on a fixed tripod at one of the receive sites, or it could be inserted into a modified garden cart for portable measurements (see Fig. 2(a)). In addition, the receiving sites contained a spectrum analyzer, computer, associated cabling (see Fig. 2(d)), and in some cases, a global positioning system (GPS) receiver (see Fig. 2(c)).

The second series of experiments used the omnidirectional discone antennas in Fig. 2(b), with the same receiver configuration as in Fig. 2(d) and antenna heights of 2 to 3 meters. The discone antennas had a gain of 2 dBi and a beamwidth of approximately 45 degrees. Horn antennas in Fig. 2(b) were used for the 2.4 GHz and 4.9 GHz frequency bands in later experiments. The gain was 10 dBi and a beamwidth of approximately 45 degrees at the frequencies of interest.

As shown in Fig. 2, the measurement system consisted of a portable spectrum analyzer controlled by a graphical programming language. The software ran parallel processes of collecting, processing, and saving the data for post-collection processing. The data were continuously read from the spectrum analyzer and stored in data buffers. These buffers were read and processed for each signal and displayed for operator viewing.

TABLE IV
LIST OF STRUCTURES IN THE EXPERIMENTS

| Number | Structure |
|---|---|
| i | New Orleans Apartment, LA |
| ii | Philadelphia Sports Stadium, PA |
| iii | † Office Building, Phoenix, AZ |
| iv | Colorado Springs Hotel Complex, CO |
| v | Grocery Store, Boulder, CO |
| vi | NIST Office, Gaithersburg, MD |
| vii | Shopping Mall, Bethesda, MD |
| viii | Discovery Office, Silver Spring, MD |
| ix | Washington DC Convention Center |
| x | ‡Horizon West Apartment, Boulder, CO |
| xi | ‡Oil Refinery, Commerce City, CO |
| xii | ‡NIST Laboratory, Boulder, CO |
| † Only 150 and 900 MHz bands measured<br>‡ Time domain and modulated signals covered in [12] | |

The processed data were then stored in additional buffers to be re-sorted and saved to a file on disk.

The sampling rate of the complete measurement process was the major factor in how much spatial resolution we had during radio-mapping experiments and the time resolution for recording the signals. (We also had some flexibility in our walking speed.) Over the course of this multiple year effort, we used three different models of spectrum analyzers, with different sampling rate capabilties. As mentioned above, the slow sampling rate for the first four experiments primarily arose from collecting data for all frequencies during a single walk-through. For the remaining eight experiments, only a single frequency was collected during each walk-through, resulting in an immediate increase in sampling rate by a factor of approximately eight. Further software and parameter optimization allowed the latter experiment sampling rates of between 0.2 to 0.3 s.

## III. BUILDING DESCRIPTIONS

Table IV lists the large structures tested, which include four office buildings, two apartment buildings, one hotel, one grocery store, one shopping mall, one convention center, one sports stadium, and one oil-refinery. This section briefly describes three of the twelve different structures, while descriptions and pictures of all the structures are given in [13].

### A. Philadelphia Sports Stadium

The nearly circular stadium was constructed of reinforced concrete, steel, and standard interior finish materials. The stadium was scheduled for demolition via implosion later that week. Fig. 3 shows the stadium with some of the implosion preparations and partial demolition of different sections. As depicted in these figures, the stadium had multiple levels with large open areas. The exterior perimeter of the stadium was approximately 805 m (1/2 mile). Since this structure was also scheduled for implosion, significant demolition was already completed when we arrived; all plumbing fixtures, most glass windows and doors, and other contents had been removed.

Fig. 3. Pictures of the Philadelphia sports stadium.

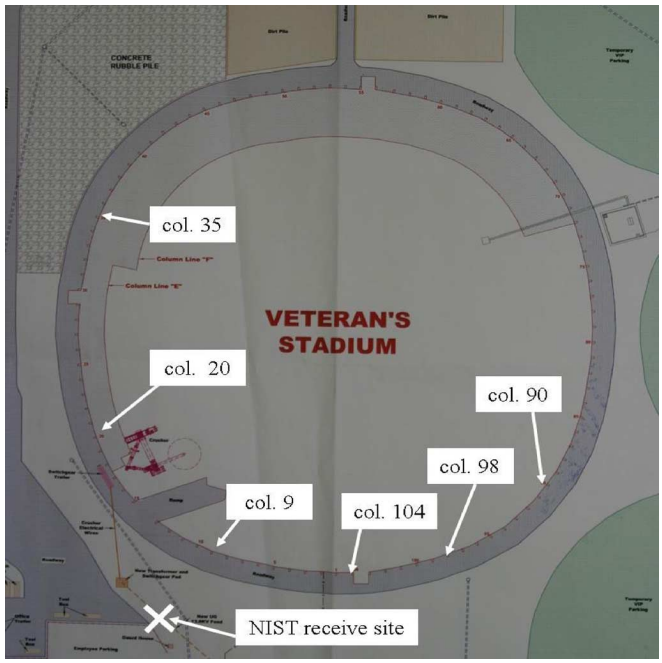


Fig. 4. Plan view of the Philadelphia sports stadium (Veteran's Stadium).

Material had been judiciously removed from certain structural parts of the lower levels including stairwells and elevator shafts to facilitate a proper collapse during the implosion. Fig. 4 shows a plan of the structure and approximate locations of the receive site. Measurements performed during and after the implosion are reported in [7].

Fig. 5. Pictures of the Washington DC Convention Center. The two lower pictures show two of the three receive sites.

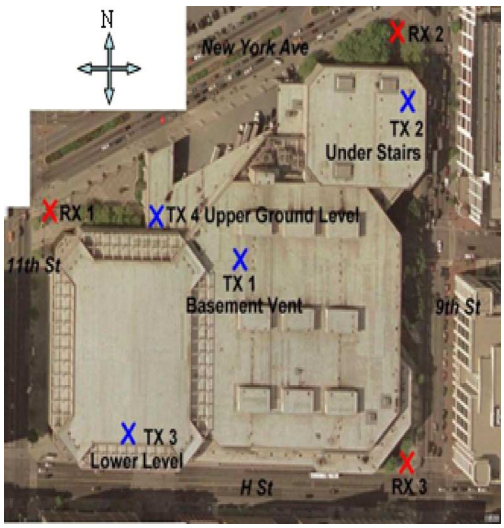


Fig. 6. Topological view of the Washington DC Convention Center. Note that receive site 3 is located at the southeast corner.

### B. Washington DC Convention Center

This massive two-level structure was constructed of reinforced concrete, steel, and standard interior finish materials. Fig. 5 shows the exterior of the convention center and two of the three receive sites. The convention center had two large levels with three levels of offices. This structure was scheduled for demolition, and significant demolition was already completed when we arrived; all plumbing fixtures, most glass windows and doors, and other contents had been removed.

Three fixed receiving sites, depicted in Fig. 6 were located on the perimeter of the convention center. Receiving site RX 1 was placed approximately 23 m (75 ft) from the northwest perimeter of the convention center. Receiving site RX 2 was placed approximately 23 m (75 ft) from the northeast perimeter of the convention center. Receiving site RX 3 was placed approximately 15 m (50 ft) from the southeast corner of the convention center. During radio mapping experiments the transmitters were carried throughout the convention center at various levels. Measurements were performed with the receiving antennas polarized in the vertical direction (with respect to the ground). The transmitter labels (TX) on Fig. 6 locate the static placement for the implosion experiment discussed in [8].

Fig. 7. Pictures of the "interior" of the Commerce City oil refinery. The picture in the bottom right-hand corner was taken from the top of a tower.

### C. Commerce City, Colorado Oil Refinery

The refinery (Fig. 7), was basically an outdoor facility with several intricate piping systems. Measurements were performed during daytime hours and, as a result, people were moving throughout the refinery. During the measurement, the transmitters were carried throughout the dense piping systems and driven around the large metal storage tanks. The results here are only for the walk through the dense piping; [13] includes the results for the path through the storage tank area.

Fig. 8 depicts the path of the walk-through and the two receive sites. For the radio mapping experiments, two fixed receiving sites (as described above) were assembled on the south side and north side of the refinery complex (see Fig. 8), approximately 100 m and 30 m from the piping structures. The arrows in the figure represent the actual paths that were walked. Measurements were performed with the receiving antennas polarized in the vertical direction. As the received signals were recorded, the location of the transmitters in the refinery complex was also recorded.

## IV. Summary of Experimental Results

### A. Data Presentation and Analysis

In the complete report [13] the measured data are presented from several perspectives. Plots of the radio-mapping data, normalized to a reference point, are provided for the investigated

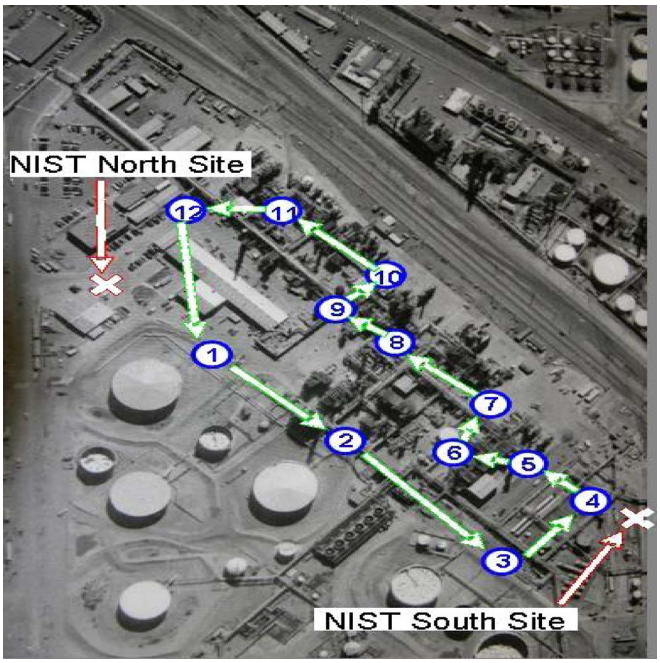


Fig. 8. Path of walk through the Commerce City oil refinery. The transmitters were carried on a round trip path up a tower from the base at position 8.

TABLE V
2.4 GHz FREQUENCY BAND STATISTICS

| Stucture/ Location | Freq. (GHz) | Ref. (dBm) | Median (dB) | $\mu$ (dB) | $\sigma$ (dB) |
|---|---|---|---|---|---|
| Apartment Building | | | | | |
| Receiver site 1 | 2.445 | -55.6 | -17.9 | -17.5 | 12.0 |
| Receiver site 2 | 2.445 | -61.0 | -25.6 | -24.8 | 9.6 |
| Oil Refinery | | | | | |
| South receive site | 2.445 | -32.0 | -52.0 | -48.3 | 16.1 |
| North receive site | 2.445 | -28.5 | -43.1 | -41.1 | 17.5 |
| NIST Lab (Boulder) | | | | | |
| Receiver site 1 | 2.445 | -18.4 | -61.9 | -62.7 | 21.1 |
| Receiver site 2 | 2.445 | -52.4 | -46.3 | -39.1 | 13.7 |
| Ref. = reference value, $\mu$ = mean, $\sigma$ = standard deviation | | | | | |

frequencies, and the radio-mapping data statistics are also included. [13] contains a series of tables that summarizes the processed data by frequency bands and buildings. This allows easier comparisons between results from different building or structure types. Table entries include a building or structure identifier, the actual frequency tested, the specific reference value $P^{\text{ref}}$, used to normalize that particular data set, and the median, mean $\mu$, and standard deviation $\sigma$, for the normalized data. For example, Table V replicates the 2.4 GHz table in [13].

The spectrum analyzers and laptops collect the raw received power $P^{\text{rec}}$, but the subsequent processing is performed on the normalized received power $P^{\text{norm}}$. Only the samples collected during the actual walk-throughs were used, i.e., the $N$ samples collected while in the process of covering the prescribed path. The normalized power is calculated as

$$P^{\text{norm}}(\text{dB}) = P^{\text{rec}}(\text{dBm}) - P^{\text{ref}}\ (\text{dBm}). \tag{1}$$

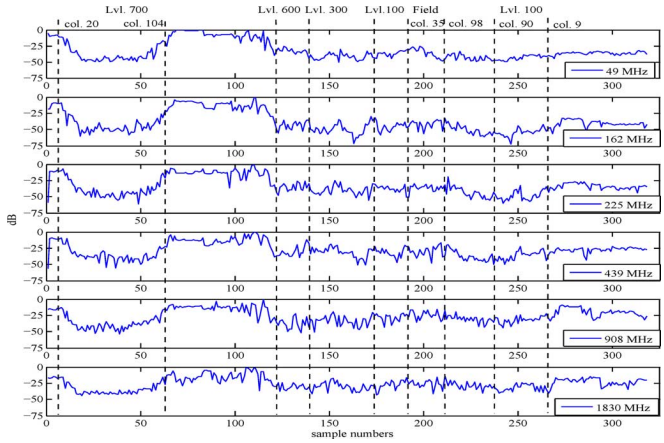


Fig. 9. Plots of the received signal level for the Philadelphia Stadium radio-mapping.

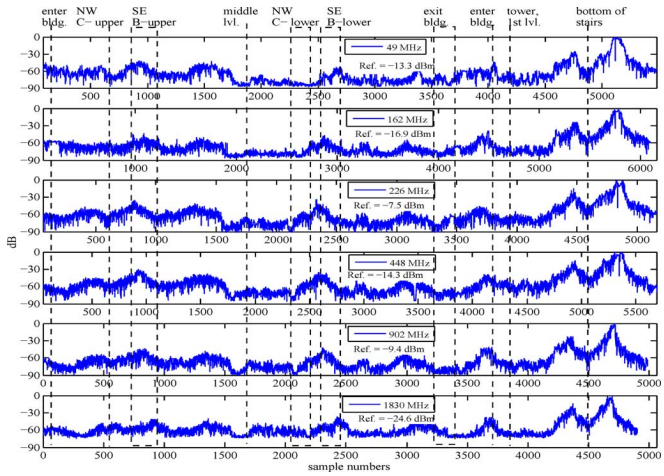


Fig. 10. Plots of the received signal level at receive site 3 during the DC Convention Center radio-mapping.

The mean and standard deviation are found from

$$\mu = \frac{\sum_{i=1}^{N} P_i^{\text{norm}}}{N} \quad (\text{dB}) \tag{2}$$

and

$$\sigma = \sqrt{\frac{1}{(N-1)} \sum_{i=1}^{N} (P_i^{\text{norm}} - \mu)^2} \quad (\text{dB}) \tag{3}$$

respectively.

Figs. 9 – 11 show radio-mapping data for the three buildings discussed above. The labels on the vertical dashed lines indicate the approximate physical location within the structure for the sample point. For the case of the stadium, (Fig. 9), the data were collected on a single walk-through for all six of the measured frequencies, and hence the vertical location markers line up almost exactly. Since the convention center and the oil refinery used a separate walk-through for each frequency, the locations

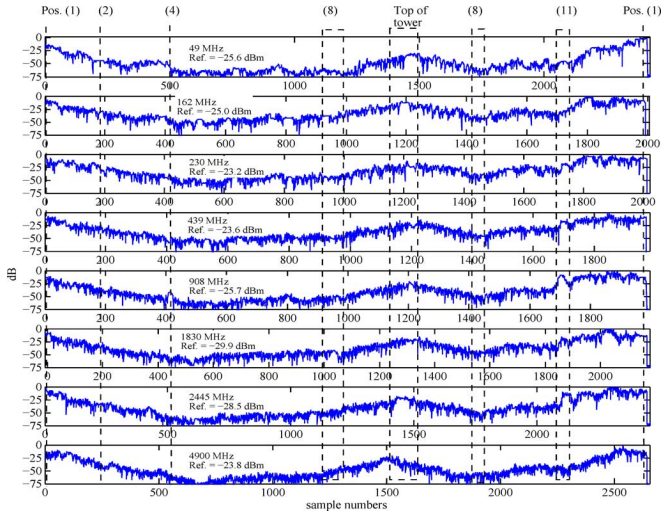


Fig. 11. Plots of the received signal level at the North receive site for the Commerce City oil refinery radio-mapping.

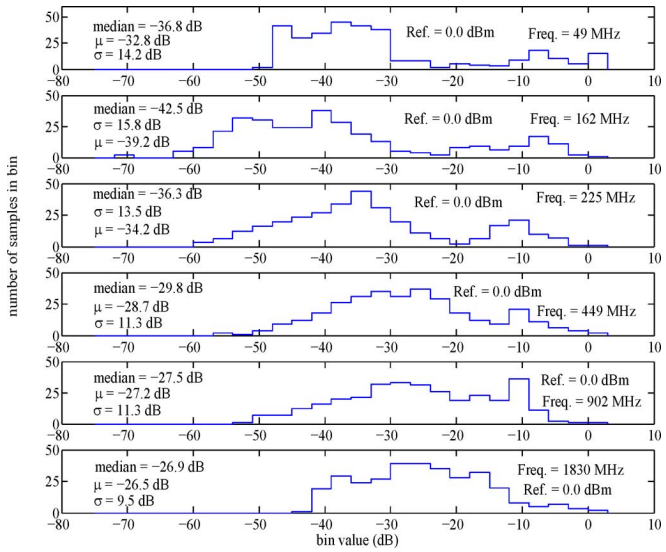


Fig. 12. Histogram and statistics for the Philadelphia stadium. 3 dB bin widths are used for histogram calculation. Note that the data were normalized during the initial collection process; hence all reference values are 0 dBm.

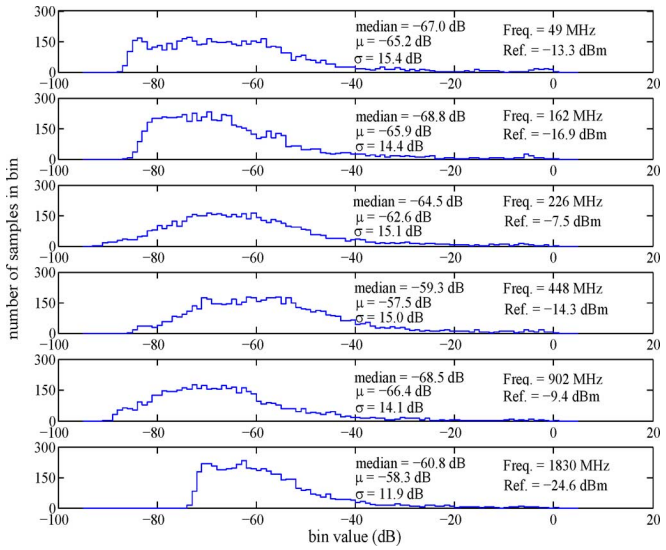


Fig. 13. Histogram and statistics for the DC Convention Center. 1 dB bin widths are used for histogram calculation.

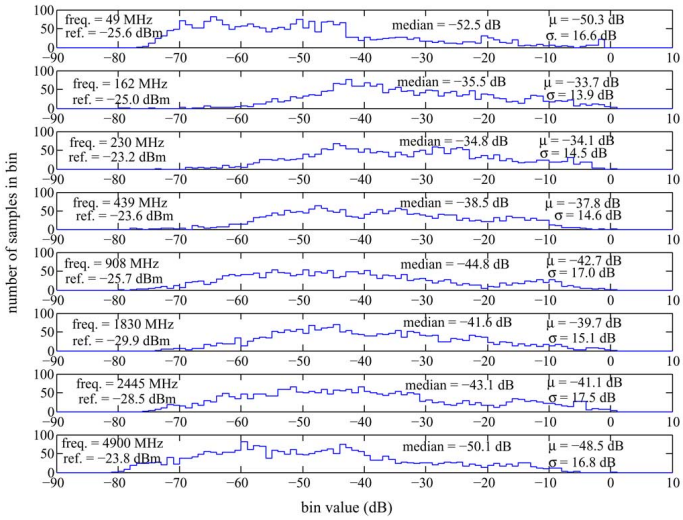


Fig. 14. Histogram and statistics for the oil refinery. 1 dB bin widths are used for histogram calculation.

are not always precisely lined up. Thus, for some of the locations a box or region is outlined to include the corresponding sample point across all frequencies. For example, in Fig. 11 the "top of tower" box includes the sample point corresponding to the top of the tower for all eight frequencies.

Figs. 12 – 14 are histograms for the walk-through data shown in Figs. 9 – 11. These histograms may be viewed as approximating the probability density function (PDF) associated with the data normalized to the reference value (ref.). Also included on the plots are the corresponding mean $\mu$, and standard deviation $\sigma$.

### *B. Discussion of Aggregate Results*

It is impractical to present all the experimental results here, due to the vast amount of data collected from multiple receivers at the twelve different sites. However, the next three graphs are helpful in examining some general trends in the complete set of collected data. (We excluded the first receiver site for the NIST laboratory in Boulder due to an excessive amount of data collected at the noise floor caused by limitations of the receive equipment.) Fig. 15 plots statistics calculated on the standard deviation across the results from all twelve buildings on a per-frequency basis. In other words, the standard deviation is calculated for a data set generated at a particular receiver site for a specific building at a single frequency, e.g., DC Convention Center at 162 MHz. The results in Fig. 15 are taken from the aggregate of all the experiments. The mean and median of $\sigma$ are calculated by including all the values at a particular frequency, e.g., 49 MHz. The maximum and minimum refer to a single radio-mapping, e.g., 49 MHz at the DC Convention Center receive site 3. These standard deviation results show that the median and mean are between 11 and 14 dB across all frequencies. Thus, the average variability is fairly constant across the

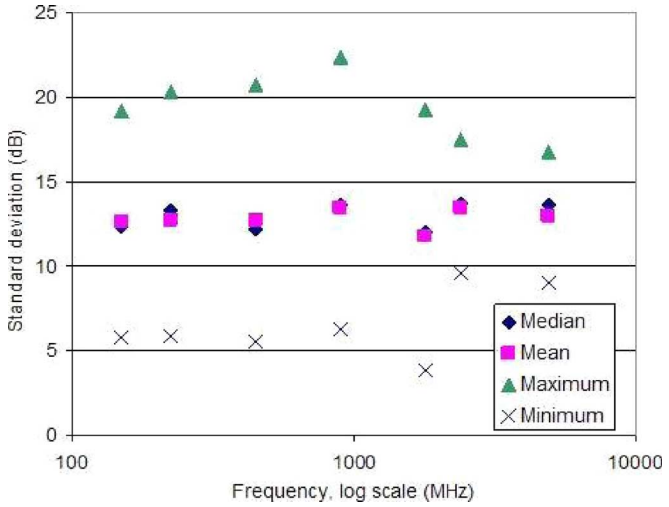


Fig. 15. Statistics of the standard deviation calculated per frequency across all twelve structures.

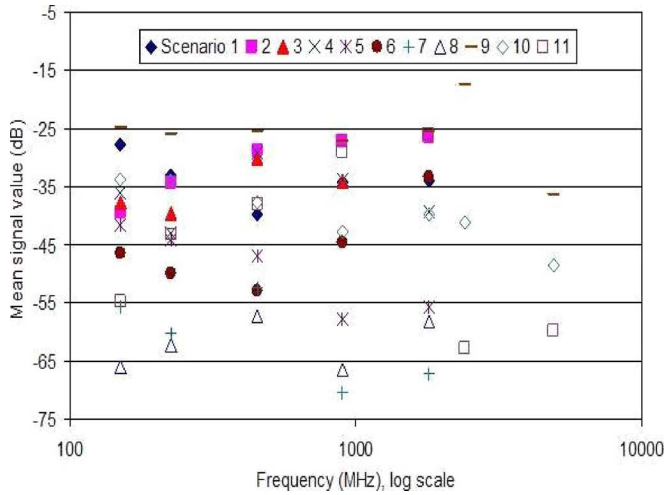


Fig. 16. Mean values of scenarios listed in Table VI.

TABLE VI
SELECTED TEST SCENARIOS

| No. | Test Scenario |
|---|---|
| 1 | New Orleans Apartment |
| 2 | Philadelphia Stadium: Inside walk-through; vertical polarization |
| 3 | Colorado Springs Hotel: $1^{st}$ walk-through; receive site 1 |
| 4 | Grocery Store, Boulder |
| 5 | NIST Office, Gaithersburg |
| 6 | Shopping Mall, Bethesda: receive site 1 |
| 7 | Discovery Office, Silver Spring |
| 8 | Washington DC Convention Center: receiver site 3 |
| 9 | Horizon West Apartment, Boulder: receive site 1 |
| 10 | Oil Refinery, Commerce City; walk-through, north receive site |
| 11 | NIST Laboratory, Boulder: receive site 1 |

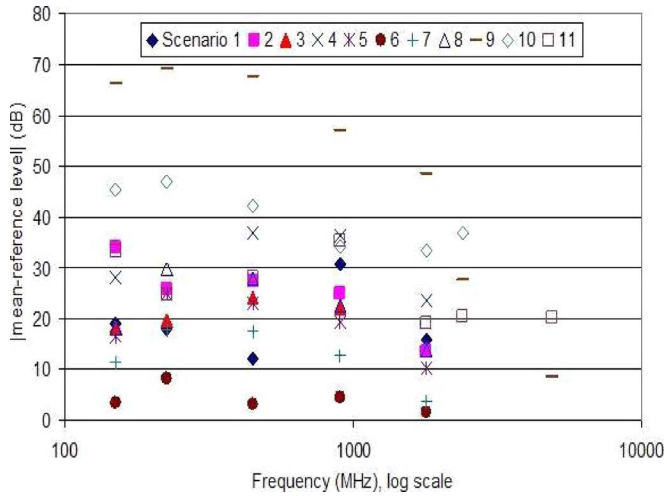


Fig. 17. Difference between mean values and reference level for scenarios listed in Table VI.

frequency bands. Note that only three structures were tested at 2.445 and 4.9 GHz.

For a coarse insight into the attenuation behavior, we examine mean values for eleven of the test scenarios listed in Table VI. (A limited number of frequencies were covered for the Phoenix office building, and thus no scenario is taken from that experiment set.) Each scenario uses the receive site at the structure location that typically provided the greatest range of received signal levels so as to reduce the impact of the test equipment dynamic range on the statistics. Note that the combination of the reference value and the dynamic limitations of the test equipment can skew the statistics. [22] uses median values instead of mean values to reduce the impact of equipment limitations.

Fig. 16 shows the mean values of the various frequencies for eleven scenarios listed in Table VI. The receiver noise floor provides an approximate value for the usable dynamic range. To obtain a rough idea of how close the mean signal is to the noise floor, we compute the difference between the mean signal level and the noise floor. Results for the eleven scenarios are shown in Fig. 17. In general, a greater difference implies less impact on the statistical results due to measured values at or below the noise floor. For example, the results for scenario six indicate mean signal levels very near the receiver noise floor, as indicated by a difference of less than 10 dB for all the frequencies. In contrast, scenario ten indicates at least a 23 dB separation between the mean signal level and the noise floor for all frequencies. Fig. 18 provides the median values for the eleven scenarios listed in Table VI, which are quite similar to the results in Fig. 16.

### C. Discussion on General Trends

The discussion here is based both on the data presented in this paper, as well as additional data presented in [13]. Any conclusion based on material unique to either publication is duly noted.

First, examination of the standard deviation results in Fig. 15 yields some interesting insights. In particular, we see that the average standard deviation for the six lower frequency bands ranges from 11.8 to 13.4 dB . Only the three latter experiments collected data at 2.445 GHz and 4.9 GHz, but those results also lie in the same range at 13.5 dB and 12.95 dB, respectively. Across all eight frequency bands, the range of maximum

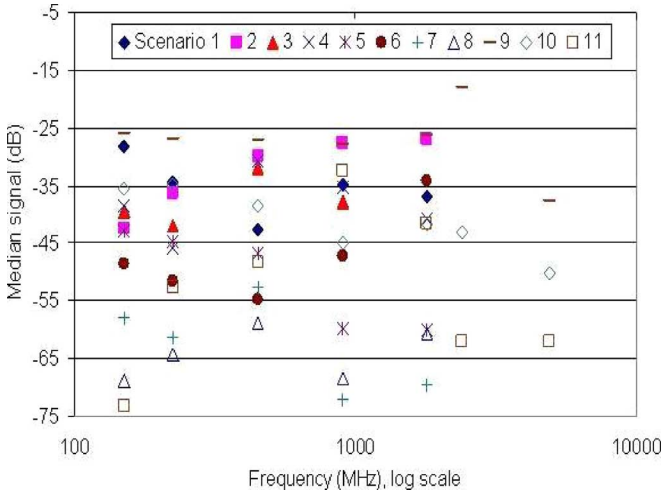


Fig. 18. Median values of scenarios listed in Table VI.

$\sigma$ varies from 16.8 to 22.3 dB, with 22.3 dB occurring at 900 MHz. The minimum $\sigma$ values range from 3.9 to 9.6 dB, with 3.9 dB occurring at 1.8 GHz.

Second, in almost all cases, the median value for the power received is 2 to 3 dB less than the average power received. The trend is clearly evident in the median and mean values listed in Figs. 12 – 14, as well as additional similar plots in [13]. This suggests that the median value may be a better measure for representing the general behavior of the building, or at least a more conservative performance measure. Use of the median is also suggested in [22].

Third, the histograms (which approximate PDFs) and the empirical cumulative density functions (see Figs. 12 – 14 and [13]) do not appear to follow any typical density function. To some extent, each individual test case will generate a unique density. However, the data do not seem to suggest an obvious average or best approximation density that could be used to collectively represent the buildings. One of the likely contributing factors is that the data collected do not have the free-space path loss due to distance removed from the data. Rician and Rayleigh distributions are used in the context of data with the path loss impact already removed from the data. However, for an emergency responder in a large building, the impact due to the size of the structure can be as important as the losses due to local scattering and multipath. Another possible contributor to the variability in distributions is that the receive sites and antenna are located as representative of an emergency response situation, i.e., close to the structures with an antenna less than 5 m above the ground. This is significantly different than the often used cell-tower measurement configuration.

## V. Conclusion

Differences in building types make it difficult to provide very strong general conclusions based on the collected data. However, we can observe some general trends in the data. The average standard deviation was between approximately 12 to 13.5 dB across the tested frequencies, which is indicative of a consistent variability in the received signal level. However, the differences in the histograms do not indicate an obvious density function for designing communication systems for such environments. Since the experiments were intended as representative of actual emergency responder behavior, (e.g., a firefighter walking through the stairwells and hallways), the radio mapping results clearly point out the challenges in designing a communication system that is well-suited to a wide range of large structures.

This paper is based on the fourth in a series of reports detailing experiments performed by NIST in order to better understand the emergency responder's radio propagation environment. The first three reports covered implosion experiments performed in three different building structures. In addition, ongoing NIST experiments are simulating and testing the performance of *ad-hoc* networks in various building structures. The ultimate goal of this paper and supporting reports is to provide system designers and wireless communication engineers with greater insight into this challenging RF propagation environment.

## References

[1] "Statement of Requirements: Background on public safety wireless communications," The SAFECOM Program, Dept. Homeland Security, 2004, vol. 1.

[2] M. Worrell and A. MacFarlane, Phoenix Fire Dept. Final Report," Phoenix Fire Department Radio System Safety Project, 2004 [Online]. Available: http://www.ci.phoenix.az.us/FIRE/radioreport.pdf

[3] "9/11 Commission Report," National Commission on Terrorist Attacks Upon the United States, 2004.

[4] "Final report for September 11, 2001 New York World Trade Center terrorist attack," Wireless Emergency Response Team (WERT), 2001.

[5] C. L. Holloway, G. Koepke, D. Camell, K. A. Remley, D. F. Williams, S. Schima, S. Canales, and D. T. Tamura, "Propagation and detection of radio signals before, during and after the implosion of a thirteen story apartment building," Boulder, CO, 2005, NIST Tech. Note 1540.

[6] C. L. Holloway, G. Koepke, D. Camell, K. A. Remley, and D. F. Williams, "Radio propagation measurements during a building collapse: applications for first responders," in *Proc. Int. Symp. Advanced Radio Tech.*, Boulder, CO, Mar. 2005, pp. 61–63.

[7] C. L. Holloway, G. Koepke, D. Camell, K. A. Remley, D. F. Williams, S. Schima, and D. T. Tamura, "Propagation and detection of radio signals before, during and after the implosion of a large sports stadium (Veterans' Stadium in Philadelphia)," Boulder, CO, 2005, NIST Tech. Note 1541.

[8] C. L. Holloway, G. Koepke, D. Camell, K. A. Remley, D. F. Williams, S. Schima, M. McKinely, and R. T. Johnk, "Propagation and detection of radio signals before, during and after the implosion of a large convention center," Boulder, CO, 2006, NIST Tech. Note 1542.

[9] "APCO Project 25 Standards for Public Safety Digital Radio," APCO International, Aug. 1995 [Online]. Available: http://www.apcointl.org/frequency/project25/information.html

[10] P. Whitehead, "The other communications revolution [TETRA standard]," *IEE Rev.*, vol. 42, no. 4, pp. 167–170, Jul. 1996.

[11] C. Edwards, "Wireless – Building on tetra," *Eng. Technol.*, vol. 1, no. 2, pp. 32–36, May 2006.

[12] K. A. Remley, G. Koepke, C. L. Holloway, C. Grosvenor, D. Camell, J. Ladbury, R. T. Johnk, D. Novotny, W. F. Young, G. Hough, M. D. McKinley, Y. Becquet, and J. Korsnes, "Measurements to support modulated-signal radio transmissions for the public-safety sector," Boulder, CO, 2008, NIST Tech. Note 1546.

[13] C. L. Holloway, W. Young, G. Koepke, D. Camell, Y. Becquet, and K. A. Remley, "Attenuation of radio wave signals coupled into twelve large building structures," Boulder, CO, 2008, NIST Tech. Note 1545.

[14] D. M. J. Devasirvatham, C. Banerjee, R. R. Murray, and D. A. Rappaport, "Four-frequency radiowave propagation measurements of the indoor environment in a large metropolitan commercial building," in *Proc. GLOBECOM*, Phoenix, AZ, Dec. 2–5, 1991, pp. 1282–1286.
[15] K. M. Ju, C. C. Chiang, H. S. Liaw, and S. L. Her, "Radio propagation in office building at 1.8 GHz," in *Proc. 7th IEEE Int. Symp. on Personal, Indoor and Mobile Radio Communications*, Taipei, Oct. 15–18, 1996, pp. 766–770.
[16] T. N. Rubinstein, "Clutter losses and environmental noise characteristics associated with various LULC categories," *IEEE Trans. Broadcasting*, vol. 44, no. 3, pp. 286–293, Sep. 1998.
[17] J. H. Tarng and D. W. Perng, "Modeling and measurement of UHF radio propagating through floors in a multifloored building," *Proc. Inst. Elect. Eng. Microw. Antennas Propag.*, vol. 144, no. 5, pp. 359–363, Oct. 1997.
[18] L. P. Rice, "Radio transmission into buildings at 35 and 150 mc," *Bell Syst. Tech. J.*, pp. 197–210, Jan. 1959.
[19] E. Walker, "Penetration of radio signals into building in the cellular radio environment," *Bell Syst. Tech. J.*, vol. 62, no. 9, Nov. 1983.
[20] W. J. Tanis and G. J. Pilato, "Building penetration characteristics of 880 MHz and 1922 MHz radio waves," in *Proc. 43th IEEE Veh. Technol. Conf.*, Secaucus, NJ, May 18–20, 1993, pp. 206–209.
[21] L. H. Loew, Y. Lo, M. G. Lafin, and E. E. Pol, "Building penetration measurements from low-height base stations at 912, 1920, and 5990 MHz," National Telecommunications and Information Administration, 1995, NTIA Rep. 95-325.
[22] A. Davidson and C. Hill, "Measurement of building penetration into medium buildings at 900 and 1500 MHz," *IEEE Trans. Veh. Technol.*, vol. 46, pp. 161–168, Feb. 1997.
[23] A. F. De Toledo, A. M. D. Turkmani, and J. D. Parsons, "Estimating coverage of radio transmissions into and within buildings at 900, 1800, and 2300 MHz," *IEEE Personal Commun.*, vol. 5, no. 2, pp. 40–47, Apr. 1998.
[24] E. F. T. Martijn and M. H. A. J. Herben, "Characterization of radio wave propagation into buildings at 1800 MHz," *IEEE Antennas Wireless Propag. Lett.*, vol. 2, pp. 122–125, 2003.
[25] A. Chandra, A. Kumar, and P. Chandra, "Propagation of 2000 MHz radio signal into a multistoryed building through outdoor-indoor interface," in *Proc. IEEE 14th Personal, Indoor and Mobile Radio Communications PIMRC 2003*, Sep. 2003, vol. 3, pp. 2983–2987.
[26] R. J. C. Bultitude, Y. L. C. de Jong, J. A. Pugh, S. Salous, and K. Khokhar, "Measurement and modelling of emergency vehicle-to-indoor 4.9 GHz radio channels and prediction of IEEE 802.16 performance for public safety applications," in *Proc. IEEE 65th Vehicular Technology Conf. VTC2007-Spring*, Apr. 2007, pp. 397–401.
[27] M. Karam, W. Turney, K. Baum, P. Satori, L. Malek, and I. Ould-Dellahy, "Outdoor-indoor propagation measurements and link performance in the VHF/UHF bands," in *Proc. IEEE 68th Vehicular Technology Conf. VTC 2008-Fall*, Sep. 2008, pp. 1–5.
[28] S. R. Saunders, K. Kelly, S. M. R. Jones, M. Dell'Anna, and T. J. Harrold, "The indoor-outdoor radio environment," *Electron. Commun. Eng. J.*, vol. 12, no. 6, pp. 249–261, Dec. 2000.
[29] D. Molkdar, "Review on radio propagation into and within buildings," *Inst. Elect. Eng. Proc.-H*, vol. 38, no. 1, pp. 61–73, Feb. 1991.

**William F. Young** (M'06) received the B.S. degree in electronic engineering technology from Central Washington University, Ellensburg, in 1992, the M.S. degree in electrical engineering from Washington State University at Pullman, in 1998, and the Ph.D. degree from the University of Colorado at Boulder, in 2006.

Since 1998, he has worked for Sandia National Laboratories in Albuquerque, NM, where he is currently a Principal Member of the Technical Staff. His work at Sandia includes the analysis and design of cyber security mechanisms for both wired and wireless communication systems used in the National Infrastructure and the Department of Defense. He has also been a Guest Researcher at the National Institute of Standards and Technology in Boulder, CO, from 2003 to 2009, and is working on improving wireless communication systems for emergency responders. His current research interests are in electromagnetic propagation for wireless systems, and the impacts of the wireless channel on overall communication network behavior.

**Christopher L. Holloway** (S'86–M'92–SM'04–F'10) was born in Chattanooga, TN, on March 26, 1962. He received the B.S. degree from the University of Tennessee at Chattanooga in 1986, and the M.S. and Ph.D. degrees from the University of Colorado at Boulder, in 1988 and 1992, respectively, both in electrical engineering.

During 1992, he was a Research Scientist with Electro Magnetic Applications, Inc., Lakewood, CO. His responsibilities included theoretical analysis and finite-difference time-domain modeling of various electromagnetic problems. From fall 1992 to 1994, he was with the National Center for Atmospheric Research (NCAR), Boulder. While at NCAR his duties included wave propagation modeling, signal processing studies, and radar systems design. From 1994 to 2000, he was with the Institute for Telecommunication Sciences (ITS), U.S. Department of Commerce in Boulder, where he was involved in wave propagation studies. Since 2000, he has been with the National Institute of Standards and Technology (NIST), Boulder, CO, where he works on electromagnetic theory. He is also on the Graduate Faculty at the University of Colorado at Boulder.

Dr. Holloway was awarded the 2008 IEEE EMC Society Richard R. Stoddart Award, the 2006 Department of Commerce Bronze Medal for his work on radio wave propagation, the 1999 Department of Commerce Silver Medal for his work in electromagnetic theory, and the 1998 Department of Commerce Bronze Medal for his work on printed circuit boards. His research interests include electromagnetic field theory, wave propagation, guided wave structures, remote sensing, numerical methods, and EMC/EMI issues. He is currently serving as Co-Chair for Commission A of the International Union of Radio Science and is an Associate Editor for the IEEE TRANSACTIONS ON ELECTROMAGNETIC COMPATIBILITY. He was the Chairman for the Technical Committee on Computational Electromagnetics (TC-9) of the IEEE Electromagnetic Compatibility Society from 2000–2005, served as an IEEE Distinguished lecturer for the EMC Society from 2004–2006, and is currently serving as Co-Chair for the Technical Committee on Nano-Technology and Advanced Materials (TC-11) of the IEEE EMC Society.

**Galen Koepke** (M'94) received the B.S.E.E. degree from the University of Nebraska, Lincoln, in 1973 and the M.S.E.E. degree from the University of Colorado at Boulder, in 1981.

He is an NARTE Certified EMC Engineer. He has contributed, over the years, to a wide range of electromagnetic issues. These include measurements and research looking at emissions, immunity, electromagnetic shielding, probe development, antenna and probe calibrations, and generating standard electric and magnetic fields. Much of this work has focused on TEM cell, anechoic chamber, open-area-test-site (OATS), and reverberation chamber measurement techniques along with a portion devoted to instrumentation software and probe development. He now serves as Project Leader for the Field Parameters and EMC Applications program in the Radio-Frequency Fields Group. The goals of this program are to develop standards and measurement techniques for radiated electromagnetic fields and to apply statistical techniques to complex electromagnetic environments and measurement situations. A cornerstone of this program has been National Institute of Standards and Technology (NIST), work in complex cavities such as the reverberation chamber, aircraft compartments, etc.

**Dennis Camell** (M'XX) received the B.S. and M.E. degrees in electrical engineering from the University of Colorado, Boulder, in 1982 and 1994, respectively.

From 1982 to 1984, he worked for the Instrumentation Directorate, White Sands Missile Range, NM. Since 1984, he has worked on probe calibrations and EMI/EMC measurements with the Electromagnetics Division, National Institute of Standards and Technology (NIST), Boulder, CO. His current interests are measurement analysis (including uncertainties) in various environments, such as OATS and anechoic chamber, and development of time domain techniques for use in EMC measurements and EMC standards. He is involved with several EMC working standards committees and is chair of ANSI ASC C63 SC1.

**Yann Becquet,** photograph and biography not available at the time of publication.

**Kate A. Remley** (S'92–M'99–SM'06) was born in Ann Arbor, MI. She received the Ph.D. degree in electrical and computer engineering from Oregon State University, Corvallis, in 1999.

From 1983 to 1992, she was a Broadcast Engineer in Eugene, OR, serving as Chief Engineer of an AM/FM broadcast station from 1989–1991. In 1999, she joined the Electromagnetics Division, National Institute of Standards and Technology (NIST), Boulder, CO, as an Electronics Engineer. Her research activities include metrology for wireless systems, characterizing the link between nonlinear circuits and system performance, and developing methods for improved radio communications for the public-safety community.

Dr. Remley was the recipient of the Department of Commerce Bronze and Silver Medals and an ARFTG Best Paper Award. She is currently the Editor-in-Chief of *IEEE Microwave Magazine* and Chair of the MTT-11 Technical Committee on Microwave Measurements.